Archives of Virology
https://doi.org/10.1007/s00705-019-04332-8

ORIGINAL ARTICLE

Impact of hepatitis B virus genotype F on *in vitro* diagnosis: detection efficiency of HBsAg from Amerindian subgenotypes F1b and F4

María J. Limeres[1] · Evangelina R. Gomez[2] · Diego G. Noseda[3] · Carolina S. Cerrudo[4] · Pablo D. Ghiringhelli[4] · Alejandro D. Nusblat[5] · María L. Cuestas[1]

Received: 9 January 2019 / Accepted: 31 May 2019

Abstract

The influence of the high genetic variability of hepatitis B virus (HBV) on the sensitivity of serological assays has received little attention so far. A major source of variability is related to viral genotypes and subgenotypes. Their possible influence on diagnosis and prophylaxis is poorly known and has mostly been evaluated for genotypes A, B, C and D. Robust data showing the detection efficiency of HBsAg from genotype F is lacking. This study examined the effect of virus-like particles containing HBsAg from genotypes A and F (particularly, F1b and F4) produced in *Pichia pastoris* in relation to the anti-HBs antibodies used in the immunoassays for *in vitro* diagnosis and compared it with that exerted by the G145R S-escape mutant. The results showed that HBsAg detection rates for subgenotypes F1b and F4 differed significantly from those obtained for genotype A and that subgenotype F1b had a major impact on the sensitivity of the immunoassays tested. Prediction of the tertiary structure of subgenotypes F1b and F4 revealed changes inside and outside the major hydrophilic region (aa 101-160) of the HBsAg compared to genotype A and the G145R variant. A phosphorylation site (target for protein kinase C) produced by the G145R substitution might prevent recognition by anti-HBs antibodies. In conclusion, the use of different genotypes or variants for diagnosis could improve the rate of detection of HBV infection. The incorporation of a genotype-F-derived HBsAg vaccine in areas where this genotype is endemic should be evaluated, since this might also affect vaccination efficacy.

Introduction

Hepatitis B virus (HBV) infection is a major cause of liver disease worldwide, with an estimated 257 million carriers who are at risk of developing liver cirrhosis and hepatocellular carcinoma (HCC) [1].

High genetic variability is a feature of HBV and plays a role in the pathogenesis and natural history of HBV infection. A major source of variability is related to viral genotypes and subgenotypes. To date, based on an intergroup genetic divergence greater than 7.5% across the entire genome sequence, HBV has been classified phylogenetically into at least 10 genotypes (A-J) [2, 3]. With an intergroup genetic divergence greater than 4% but less than 7.5% over the full-length genome and good bootstrap support, genotypes A-D and F have been further classified into at least 40 subgenotypes [4]. Lastly, based on genetic divergence

Handling Editor: Zhongjie Shi.

Electronic supplementary material The online version of this article (https://doi.org/10.1007/s00705-019-04332-8) contains supplementary material, which is available to authorized users.

✉ María L. Cuestas
marilucuestas@gmail.com

[1] CONICET, Instituto de Investigaciones en Microbiología y Parasitología Médica (IMPaM), Universidad de Buenos Aires, Buenos Aires, Argentina

[2] Instituto de Agrobiotecnología y Biología Molecular, INTA-CONICET, Buenos Aires, Argentina

[3] Instituto de Investigaciones Biotecnológicas-Instituto Tecnológico de Chascomús (IIB-INTECH), Universidad Nacional de San Martín (UNSAM)-Consejo Nacional de Investigaciones Científicas y Técnicas (CONICET), Buenos Aires, Argentina

[4] Departamento de Ciencia y Tecnología, Laboratorio de Ingeniería Genética y Biología Celular y Molecular, Área Virosis de Insectos (LIGBCM-AVI), Instituto de Microbiología Básica y Aplicada (IMBA), Universidad Nacional de Quilmes, Bernal, Provincia de Buenos Aires, Argentina

[5] Facultad de Farmacia y Bioquímica, Instituto de Nanobiotecnología (NANOBIOTEC), Universidad de Buenos Aires, Buenos Aires, Argentina

Published online: 02 July 2019

less than 4% in the whole HBV genome, some subgenotypes have been further divided into clades [4].

HBV genotypes have been shown to have a distinct geographic distribution and seem to differ in biological properties that may account for differences in the modes of transmission, disease progression, and/or clinical outcome of the infection and in the antiviral treatment or vaccination responses [5].

Genotype F, which is recognized as the most genetically divergent, is one of the less-studied HBV genotypes. It is widely distributed in Central and South America and around the Arctic Circle and has been divided into four subgenotypes (F1 to F4). F1 and F2 have been further divided into clades a and b. F1a has been described in Costa Rica and El Salvador; F1b in Alaska, Argentina and Chile; F2a in Brazil and Venezuela; F2b only in Venezuela; F3 in Colombia, Venezuela and Panama; and F4 in Bolivia, Argentina and southern Brazil [6]. It has been shown that patients infected with genotype F tend to have a more-severe progression with higher mortality rates than those infected with genotype A or D (the most globally distributed genotypes) [7, 8]. In this regard, the risk of HCC development is almost 8-fold higher for genotype F than for the other genotypes [9].

With regard to the impact of HBV genotypes on prophylaxis measures, there have been several reports of vaccination failure due to genotype complications [10]. With respect to genotype F, for instance, Tacke *et al*. reported the case of a fully immunocompetent German patient who developed acute hepatitis B following infection by HBV subgenotype F1b despite a complete and formally successful vaccination [11]. Similarly, an Irish man who was vaccinated and showed production of protective anti-HBs antibodies acquired chronic hepatitis B by subgenotype F1b [12]. It is noteworthy that neither of those patients carried HBsAg (or vaccine) escape mutants or S gene variations that could explain the vaccine failure, such as the best-documented S-escape mutant worldwide, G145R.

It should be noted that current HBV vaccines include recombinant HBsAg of subgenotype A2, subtype *adw*2, whereas all genotype F isolates belong to serological subtype *adw*4, and rarely, some F4 isolates also belong to the serological subtypes *adw2* or *ayw*4 [2]. The fact that subtype epitopes are highly immunogenic, together with the emergence of S-escape mutants, has raised questions about the effectiveness of the current vaccine, particularly in Central and South America, where genotype F is more frequent.

With regard to diagnosis, the impact of HBV genotypes on the sensitivity of HBsAg detection assays has been poorly investigated. However, careful virological analysis has suggested that current diagnostic tests might not efficiently detect infections with HBV genotype F. The amino acid sequence for the major neutralization domain (or "a" determinant) of the HBsAg from genotype F is more divergent than that from genotype A. Antibodies to epitopes within this immunogenic determinant are used in commercially available assays for HBsAg. This implies that the current diagnostic kits are not perfect and that efforts should be directed towards the development of novel diagnostic kits that efficiently detect all genotypes of HBV and even the S-escape mutants. Similar considerations should be taken into account for the development of novel anti-hepatitis B vaccines that efficiently protect against all genotypes of HBV and vaccine escape mutants.

Unfortunately, to date, there is a lack of data available on genotype F diagnosis and prophylaxis responses. This is due to the fact that the largest studies evaluating hepatitis have been conducted in Asia, Europe and the USA, where the prevalence of genotype F is very low.

In this study, we examined the effect of HBsAg from genotypes A and F (placing special emphasis on the study of the subgenotypes prevalent in the southern area of South America [subgenotypes F1b and F4]) in relation to the anti-HBs antibodies used in diagnosis and compared it with that exerted by the G145R S-escape mutant. In order to achieve this goal, all of these HBsAg variants were produced in *Pichia pastoris*, purified and tested for their ability to self-assemble into virus-like particles (VLPs). Two commercial diagnostic assays were tested to compare the detection of all these HBsAg variants, and thus their ability to bind to the specific antibodies used in diagnosis. A bioinformatic analysis and tertiary structure modeling of all these variants were also performed.

Materials and methods

Expression in *P. pastoris* and purification of VLPs containing wild-type HBsAg from subgenotypes A2, F1b, and F4 and the G145R mutant

P. pastoris strain X-33, purchased from Life Technologies Inc., was used for the expression of all of the recombinant HBsAg variants due to its advantages for generating stable strains with high expression of correctly self-assembled VLPs. To this aim, the coding sequences of wild-type HBsAg (UniprotKB ID: Q598R3) and the G145R S-escape mutant (UniprotKB ID: Q9WHR2) from subgenotype A2 as well as the coding sequences of wild-type HBsAg from subgenotypes F1b (UniprotKB ID: O57308) and F4 (UniprotKB ID: Q9YXC4), were codon-optimized for yeast expression in *P. pastoris* and were synthesized and cloned into the pPICZ A *Pichia* expression vector (Life Technologies Inc., USA) by GenScript (USA) downstream the inducible alcohol oxidase (AOX1) promoter. The expression construct was linearized with *Sac*I and used to transform competent cells for genome integration, and clones resistant to zeocin were selected. The

recombinant transformants were then cultured on minimal methanol (MM) and minimal dextrose (MD) plates to differentiate Mut+ from MutS phenotypes. For protein expression, cells were grown on a defined medium at 30 ± 1 °C [13] in a fed-batch mode as described previously [14–17], using a 6-L BioFlo 110 bioreactor (New Brunswick Scientific, USA) equipped with a BioCommand bioprocessing controller unit. Briefly, cells were first grown in a batch procedure on glycerol (initial concentration, 40 g/L). After depletion of glycerol, production of HBsAg was induced by adding 100% (v/v) methanol to a final concentration of 1% (v/v) every 24 h for 3 days to maintain induction.

The purification of recombinant HBsAg-VLPs was performed in all cases by a first step of hydrophobic adsorption/desorption on colloidal silica (Aerosil® 380, Evonik, Germany) [18, 19], followed by a second step of ultracentrifugation on double sucrose cushion at 274,000 × *g* for 2.5 h at 4 °C [20] and a third step of ultrafiltration using an Amicon® Ultra10K device (10,000 MWCO; EMD-Millipore, USA). The purification strategy is shown in Figure S1.

The identification of HBsAg was performed by liquid chromatography-mass spectrometry (LC-MS) using an Accucore TM Easy-Spray C18 analytical column (Thermo Fisher Scientific, USA) coupled to an EASY-nLCTM 1000 system. The mass spectra of peptides were acquired using an Orbitrap nLC/MS instrument. Data analysis was performed using the Thermo Proteome Discoverer program (Thermo Fisher Scientific).

The morphology of the recombinant HBsAg VLPs was examined using a Jeol 1200 EX II transmission electron microscope (TEM; Jeol, USA) operating at an acceleration voltage of 60,000 V. For that purpose, samples were deposited onto Formvar carbon-coated copper grids and negatively stained with 0.5% phosphotungstic acid solution (pH 7.0), after which the grids were air-dried and analyzed.

Binding of HBsAg from genotypes A and F to the specific antibodies used in diagnosis

To test the ability of HBsAg from genotypes A, F1b and F4 to recognize the anti-HBs antibodies used in diagnosis and compare it with that of the G145R S-escape mutant, a quantitative analysis of HBsAg was done using purified VLPs at the same protein concentration (measured by densitometry in an SDS-PAGE gel using the Image J software, U. S. National Institutes of Health) using two commercial diagnostic immunoassays: the ARCHITECT HBsAg Assay (ARCHITECT HBsAg Reagent Kit, Abbot Laboratories, USA) and the Elecsys HBsAg II assay (Cobas Kit, Roche Diagnostics, Switzerland) according to the manufacturers' instructions. Both kits have a monoclonal capture solid phase and a polyclonal detection reagent.

SDS-PAGE analysis was performed in a 12% polyacrylamide gel under denaturing and reducing conditions in the presence of 2% SDS and 0.1 M DTT, respectively. A 15-µl sample aliquot was mixed with 5 µl of 4X loading buffer and boiled for 5 min before loading on the gel. Electrophoresis was performed at 100 V, and proteins were either silver stained or stained with Coomassie brilliant blue.

For calibration, a dilution series containing 0 to 0.5 µg of HBsAg standard of genotype A2 (kindly provided by a National Biotechnological Foundation) per ml was employed. All samples were analyzed in triplicate.

Statistical significance was analyzed using Graph Pad Prism 5 software for Windows using the two-way ANOVA test. Differences were considered significant at $p < 0.05$.

HBsAg secondary and tertiary protein structure characterization

Secondary structure predictions of HBsAg genotypes A, F1b, F4 and the G145R S-escape mutant were performed using the JPRED 4 server [21], PSI/TMCoffee, PSIPRED, RHYTHM, MENSAT-SVM, and DAS-TM. Default parameters were used in all cases. Hydrophobicity and amphipathicity analyses were performed using a program designed *ad hoc* by Ghiringhelli, P.D. Briefly, individual hydrophobic and amphipathic profiles were obtained for each protein using a sliding-window strategy and a standard hydrophobicity table. Previous results were used to predict and characterize a secondary consensus structure.

In a first attempt to perform homology modeling of the three-dimensional structure of HBsAg, the Protein Data Bank (PDB) was searched using the sequence of HBsAg from genotype A (Q598R3). However, no suitable templates were obtained. Therefore, taking into account the previous results of the secondary structure analysis and literature data, homology modeling was done using the I-TASSER server [22], assigning additional secondary structure restraints and using the 2IQ4.pdb model (a theoretical structural model with four transmembrane α-helices, obtained from https://www.modelarchive.org/) as a template to guide I-TASSER modeling. The best model obtained was then evaluated and refined three times until a model with reasonable parameters and a secondary structure concordant with previous data was obtained. Finally, this structural model was used as a template on the I-TASSER server to generate the three-dimensional structures of the other proteins analyzed: F1b, F4 and the G145R S-escape mutant. The stereochemical quality of the model was assessed using three structure assessment tools: PROCHECK [23], QMEANBrane [24] and PROSA-web [25]. For high-resolution protein structure refinement, we used the ModRefiner algorithm [26]. Additionally, the PPM server [27] was used to calculate the rotational and translational positions in the membrane of the theoretical

models obtained for the transmembrane proteins analyzed. To further investigate the structural relationships of the four HBSAg proteins, we performed structural alignments using the Dali server [28] with manual inspection and adjustments. Molecular representations were produced using the UCSF Chimera package [29].

Results

Expression of recombinant HBsAg in *P. pastoris*

Recombinant HBsAg from genotypes A2, F1b and F4 as well as the HBsAg variant carrying the point mutation G145R were successfully expressed intracellularly in Mut+ strains of *P. pastoris* strain X-33.

As depicted in Fig. 1A and B, SDS-PAGE analysis of the recombinant HBsAg with silver staining showed that under denaturing conditions, the purified samples yielded two bands of approximately 55 and 25 kDa, corresponding to the dimer and monomer, respectively, of HBsAg. In some cases, higher-order oligomers were also observed. Analysis of tryptic and chymotryptic protein digests of the 25-kDa band by nLC/MS identified peptide sequences from HBsAg, thus confirming their identity. Aliquots of the purified VLPs were used for TEM analysis to ensure that all of the recombinant HBsAg variants produced herein were properly assembled into particles. As shown in Fig. 2, TEM analysis revealed the presence of characteristic spherical structures with a diameter of approximately 20.52 ± 1.78 nm, the so-called HBsAg VLPs. The presence of tubular self-organizing particles of 21.24 ± 2.41 nm was

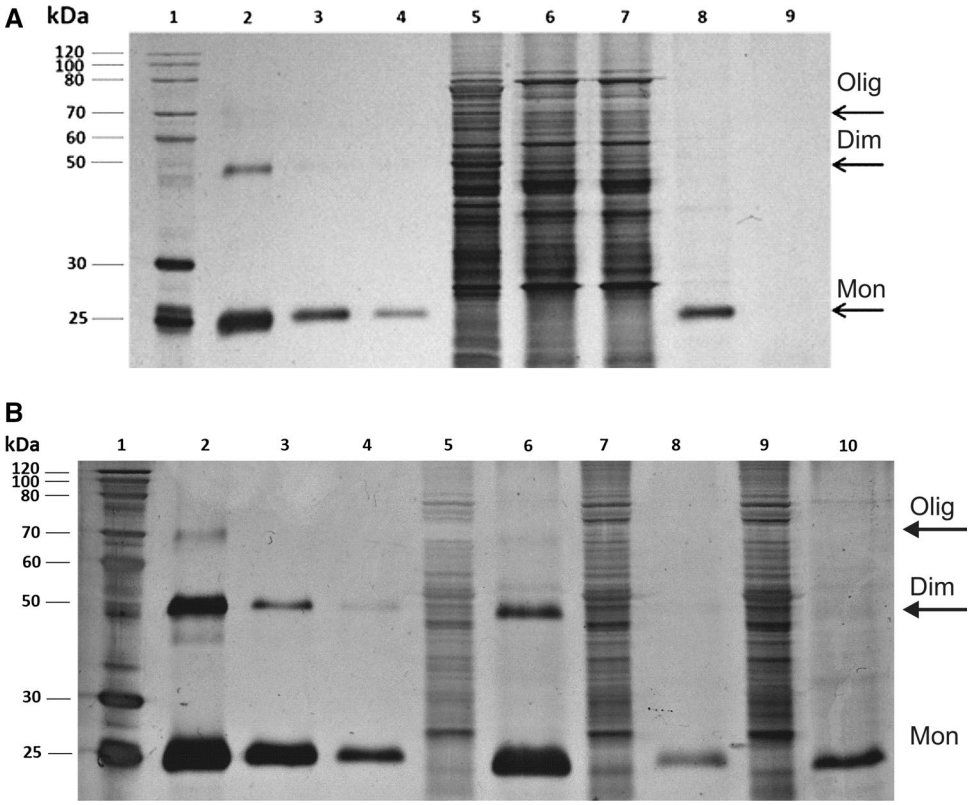

Fig. 1 **A.** Silver-stained SDS-PAGE gel of the rHBsAg fractions obtained during the purification process of WT HBsAg from genotype A, analyzed under reducing conditions. Lane 1, molecular weight protein marker; lanes 2, 3 and 4, 1, 0.5 and 0.25 µg of HBsAg standard, respectively; lane 5, crude extract prepared by disruption in breaking buffer using glass beads; lane 6, desorption with 50 mM sodium carbonate-bicarbonate buffer, pH 10.8, with 1.2 M urea for 4 h; lane 7, supernatant after ultracentrifugation on a double sucrose cushion; lane 8, purified WT HBsAg from genotype A obtained after ultrafiltration of the dialyzed samples corresponding to the VLP fraction obtained at the interface between the 25% and 70% sucrose layers after ultracentrifugation on a double sucrose cushion; lane 9, negative control. **B.** Silver-stained SDS-PAGE gel of the rHBsAg from subgenotypes F1b and F4 and from the G145R variant, analyzed under reducing conditions. Lane 1, molecular weight protein marker; lanes 2, 3 and 4, 1, 0.5 and 0.25 µg of HBsAg standard, respectively; lane 5, crude extract of HBsAg from subgenotype F1b prepared by disruption in breaking buffer using glass beads; lane 6, purified HBsAg from subgenotype F1b; lane 7, crude extract of HBsAg from subgenotype F4 prepared by disruption in breaking buffer using glass beads; lane 8, purified HBsAg from subgenotype F4; lane 9, crude extract of HBsAg G145R prepared by disruption in breaking buffer using glass beads; lane 10, purified HBsAg G145R

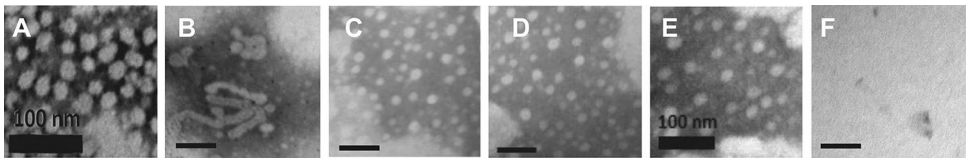

Fig. 2 Transmission electron micrographs of purified HBsAg VLPs. (**A**) and (**B**) Spherical and tubular self-organized particles, respectively, of genotype A. (**C**) subgenotype F1b. (**D**) subgenotype F4. (**E**) G145R S-escape mutant. (**F**) Negative control. Scale bar, 100 nm

observed in all rHBsAg preparations analyzed (F1b, F4, A2 and the mutant G145R).

Binding of HBsAg from genotypes A and F to specific antibodies used in diagnosis

Using the Elecsys HBsAg II assay, the rate of detection of HBsAg of genotypes F1b and F4 was 55.1% and 31.7% lower, respectively than that obtained for genotype A whereas, using the ARCHITECT HBsAg assay, the rate of HBsAg detection for the two indigenous subgenotypes was 59.5% lower and 17.9% higher, respectively, than that obtained for genotype A (Fig. 3A). HBsAg detection rates for G145R were 96.1% lower for both immunoassays than those obtained for genotype A. As shown in Fig. 3B, a significant variation (30-150%) was observed between the different commercial diagnostic assays, depending on the subgenotype. The diagnostic sensitivity for these recombinant HBsAg particles was also evaluated. For this purpose, a dilution series was made from each sample by preparing 10 HBsAg concentrations in the range of 0.1 ng/ml to 5 ng/ml. The diluent (1x PBS) served as the negative control in each dilution series of recombinant HBsAg antigens. The results showed that the sensitivity for detection of HBsAg from genotypes F1b, F4 and G145R in the Elecsys immunoassay relative to genotype A2 was 2 to 25 times lower (limit of detection, > 0.1 ng/ml for A2, > 0.3 ng/ml for F1b, > 0.2 ng/ml for F4 and > 3.0 ng/ml for G145R).

The sensitivity to HBsAg from genotypes F1b and G145R in the ARCHITECT immunoassay relative to genotype A2 was 3 to 25 times lower (limit of detection, > 0.4 ng/ml for A2, > 1.0 ng/ml for F1b and > 10.0 ng/ml for G145R), whereas F4 showed approximately two times higher sensitivity relative to genotype A2 (limit of detection, < 0.2 ng/ml).

To demonstrate that the recombinant VLPs produced in this study had correct conformational epitopes, immunoassay reactivity profiles of VLPs purified from sera of patients with chronic HBV from subgenotypes A2, F1b and F4 were compared. The results demonstrated that the recombinant VLPs had a similar reactivity to the native VLPs purified from serum samples. In both cases, a quantitative analysis of HBsAg was carried out using the purified VLPs at the same protein concentration (measured by densitometry in an SDS-PAGE gel using Image J software,) using the ARCHITECT HBsAg Assay and the Elecsys HBsAg II Assay according to the manufacturers' instructions (Fig. 4A and B).

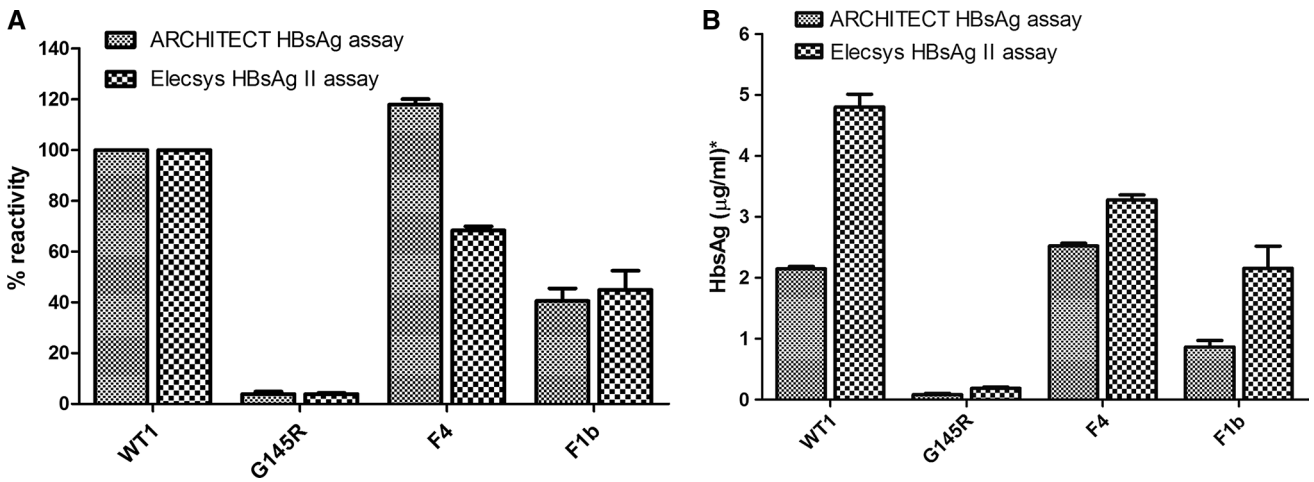

Fig. 3 Binding of recombinant HBsAg from genotypes A and F (at the same protein concentration) to specific antibodies using two commercial diagnostic immunoassays (the ARCHITECT HBsAg assay and the Elecsys HBsAg II assay). **A.** Expressed as a percentage of the reactivity of genotype A. **B.** Expressed as µg/ml using HBsAg genotype A2 for the calibration curve

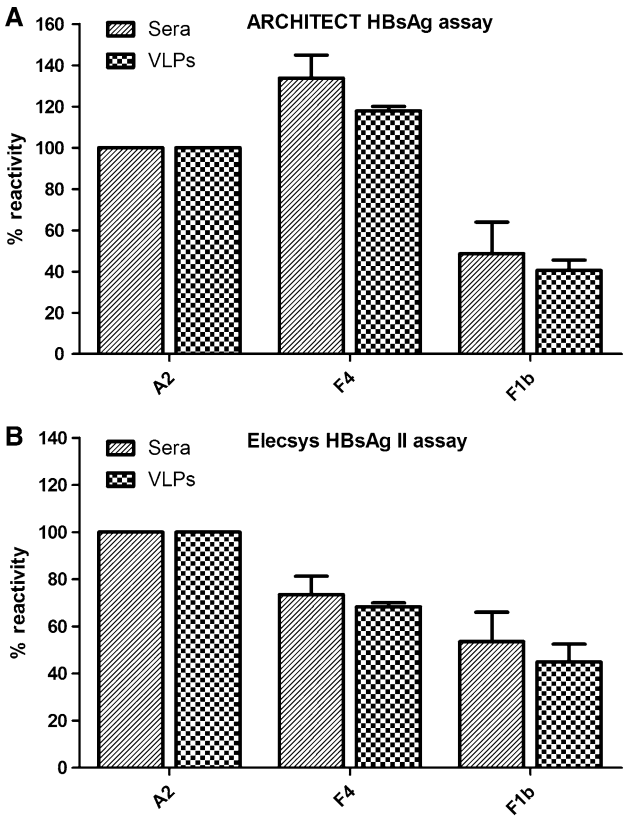

Fig. 4 Comparison of the binding ability of recombinant VLPs from genotypes A and F with the binding ability of native VLPs purified from serum samples of genotypes A and F. In both cases, a quantitative analysis of HBsAg was done using the purified VLPs at the same protein concentration (measured by densitometry analysis of the SDS-PAGE gel using Image J software), using the ARCHITECT HBsAg assay (**A**) and the Elecsys HBsAg II assay (**B**) according to the manufacturer's instructions

Secondary and tertiary structure predictions

In order to investigate amino acid sequence conservation and polymorphisms between the WT HBsAg and the other subgenotypes, the amino acid sequences of the envelope proteins were aligned using ClustalX and secondary structure elements, properties and patterns were predicted using different programs. As illustrated in Fig. 5, 29 and 28 amino acid changes were found between WT subgenotype A2 and subgenotypes F1b and F4, respectively, and only two were found between F1b and F4. Interestingly, subgenotypes F1 and F4 have 17 cysteine residues, in contrast to the 14 cysteines found in subgenotype A2. The sequence within the major hydrophilic region (MHR) was observed to be conserved, and four transmembrane alpha-helical regions were consistently predicted. Two of these helical regions, the first alpha-helix of the cytoplasmic loop and the alpha-helix of the MHR, were predicted to be amphipathic. These results enabled us to bioinformatically predict the structure of the G145R S-escape mutant. The coding sequence of the wild-type HBsAg from subgenotype A2 has a guanosine (G) at position 433, whereas the G145R S-escape mutant of the same genotype has an adenosine (A) at this position. Therefore the codon, instead of coding for glycine (G), codes for arginine (R). Thus, the G145R mutation results in the gain of a positively charged residue, which causes that region of determinant "a" to have greater accessibility to solvent. This mutation also generates a phosphorylation target for protein kinase C (PKC). Taking into account that posttranslational modifications can induce structural changes such as alterations in folding, stability, and exposure of new antigenic epitopes, phosphorylation at this site could prevent recognition of the protein by antibodies.

To investigate the effect of the amino acid sequence variability of subgenotypes F1b and F4 on HBsAg conformation, the tertiary structure of these HBsAg variants, along with

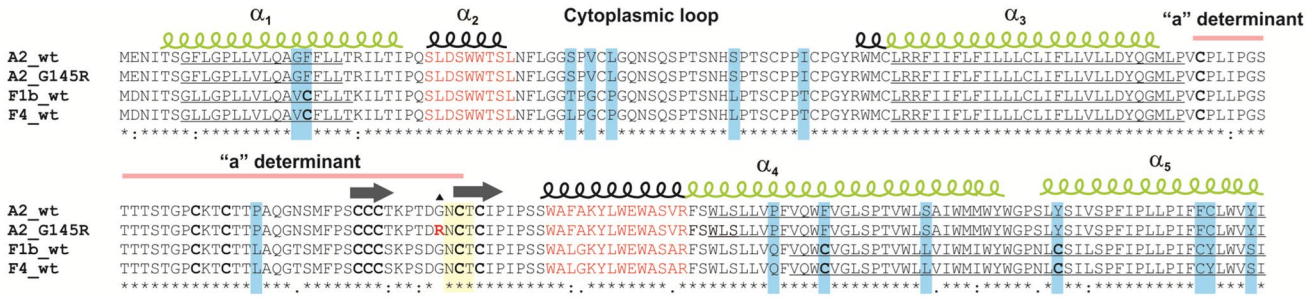

Fig. 5 Multiple sequence alignment and secondary structure prediction of HBsAg proteins. α-Helices (α_1-α_5) are indicated by squiggles, and β-sheets are indicated by arrows. Cysteines involved in disulfide bonds are indicated in bold. Extra Cys residues present in genotypes F1b and F4 are shown in bold on a blue background. The mutated residue of the G145R S-escape mutant (A2_G145R) is in bold and red, transmembrane regions are in green, and residues of the α-helical regions predicted to be amphipathic are in red. The N-glycosylation site is shown in yellow. Non-conservative changes between the A2 genotype and the F1b and F4 genotypes are shown in blue. Stars, periods and colons in the column of the alignment represent identity and conservative changes. The cytoplasmic region and "a" determinant are also indicated

the G145R S-escape mutant and the wild-type genotype A, was predicted using I-TASSER following the steps described in the Materials and methods section. All of the models that were generated were analyzed individually to determine the putative topology in the context of a eukaryotic membrane; however, for reasons of space, only the HBsAg A2 wild-type protein inserted in the membrane is shown (Fig. 6A). A comparison of all four structural models is shown in Fig. 6B, and pairwise comparisons are shown in Fig. 6D to G.

The quality of the theoretical models was evaluated using the online QMEANBrane, PROCHECK and PROSA-web programs (Fig. 6C). PROCHECK uses Ramachandran statistics to predict the percentage of residues present in different regions (core, allowed, generally allowed, and disallowed) and the goodness factor (G factor). The PROSA-web program calculates the PROSA Z-score of the structure, which is representative of model quality and is compared with the range of scores usually found in proteins of similar size. QMEANBrane was used because this program estimates the model quality using specific methods for membrane proteins. The PROCHECK analysis of four HBsAg protein models showed that the number of total residues found in the core and allowed regions was higher than 97.8% and in all cases were in good agreement with the expected value (> 90%), whereas the number of residues predicted to be in the disallowed regions was considered acceptable (< 1.6%). The G factor indicates how atypical the dihedral angles or the main-chain covalent forces are. The G values for the four models were > -0.98, whereas values < -1.0 would be considered highly unusual. All models had a range of PROSA Z-scores between -3.05 and -2.82, with acceptable values for proteins of a similar size ranging from -10 and 0 according to X-ray and NMR studies. As PROCHECK and PROSA are based on the complete PDB data set (which contains more globular proteins than membrane proteins), we also used QMEANBrane, which is based only on membrane proteins, to analyze the theoretical models. The results obtained with this program indicated that all four models have a membrane insertion energy that is within the range expected for transmembrane structures. Furthermore, Z-score values between -5.1 and -4.1 were obtained for all models (standard values range between -6 and 2). The overall results obtained by the different methods showed good results for the four models built using I-TASSER, suggesting that they were reliable for further studies. In addition, all models were used to perform local structural alignments and to identify regions of lesser

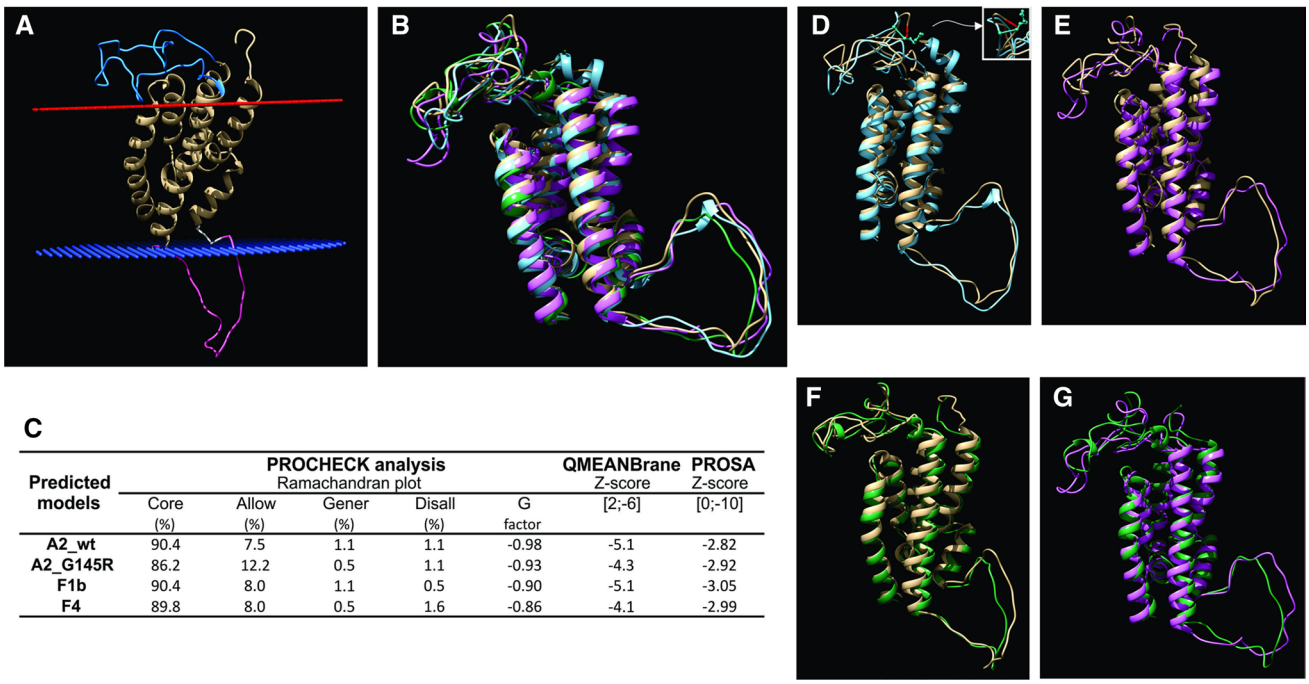

C

Predicted models	PROCHECK analysis Ramachandran plot					QMEANBrane Z-score	PROSA Z-score
	Core (%)	Allow (%)	Gener (%)	Disall (%)	G factor	[2;-6]	[0;-10]
A2_wt	90.4	7.5	1.1	1.1	-0.98	-5.1	-2.82
A2_G145R	86.2	12.2	0.5	1.1	-0.93	-4.3	-2.92
F1b	90.4	8.0	1.1	0.5	-0.90	-5.1	-3.05
F4	89.8	8.0	0.5	1.6	-0.86	-4.1	-2.99

Fig. 6 Comparison of structural models of HBsAg proteins. (**A**) Three-dimensional model of the HBSAg protein of wild-type genotype A2, showing the orientation of the protein inserted in the membrane (red, outer membrane, blue, inner membrane) is shown. In addition, the MHR motifs and the cytoplasmic loop are shown in blue and violet, respectively. (**B**) Structural alignment of the four models obtained for the proteins of genotypes A2 (white), F1b (violet), and F4 (green) and the G145R mutant protein (A2_G145R) (light blue). (**C**) Key geometric parameters used for validation of the four models. (**D**) Pairwise structure alignment of genotype A2 and mutant protein A2_G145R, with the glycine of the wild-type protein shown in red and the arginine generated by the mutation shown in ball & stick format. (**E**) Genotype F1b. (**F**) Genotype F4, using the same color code as in B. (**G**) Structural alignment of the models obtained for genotypes F1b (violet) and F4 (green)

or greater similarity between the structures. Superposition of the different variants showed that the predicted tertiary structures of subgenotypes F1b and F4 differ slightly at the global level from those of genotype A and the G145R S-escape mutant. The MHR (amino acids 101 to 160 of HBsAg, which encompassed the "a" determinant) and the other sites of amino acid variation displayed the greatest difference in RMSD values (Table 1).

Discussion

In this study, we attempted to evaluate the impact of different subgenotypes prevalent in the southern part of South America on diagnosis, and potentially on prophylaxis, of HBV infection. To diminish the global burden of hepatitis B, massive and unified efforts, such as accurate diagnosis and vaccination, are required. Epidemiological data regarding the circulating genotypes or S-escape mutants are also essential to control HBV infection, since novel diagnostic or prophylactic tools that cover all existing strains should be developed to efficiently organize all the measures to further decrease the risk of HBV infection.

In the present study, intracellular expression of HBsAg from genotypes A, F1b, and F4 and the G145R S-escape mutant was efficiently achieved in Mut+ strains of *P. pastoris* X-33. The purification of HBsAg was performed in all cases by hydrophobic adsorption/desorption on colloidal silica (Aerosil 380) followed by ultracentrifugation on a double sucrose cushion and ultrafiltration. The formation of VLPs was confirmed by TEM analysis. In all cases, uniform ~20 nm-particles were detectable. In addition to the spherical particles, short tubular structures were sometimes observed with a diameter similar to that of its spherical counterpart. According to Milhiet *et al.*, HBsAg can be produced as spherical and tubular self-organized particles when it is overexpressed in the host cell [30]. Moreover, Lündsorf *et al.* have elegantly shown that these tubular structures can be transformed into energetically more favorable VLPs under appropriate conditions [31].

HBsAg is a cysteine-rich protein with a total of 14 cysteines (out of a total of 226 amino acids) in each monomer in all genotypes except for genotypes F and H, which have 17 cysteines (out of a total of 226 amino acids). These cysteine residues have the potential to form numerous intra- and intermolecular disulfide bonds. As reported previously [18, 32–34], during the process of purification of *P. pastoris*-derived HBsAg, some disulfide bonds form spontaneously between the antigen monomers, leading to the formation of dimers or even higher-order oligomers that are visualized as a heterogeneous mixture after electrophoresis on an SDS-PAGE gel, as shown in Fig. 1A and B. These intra-chain and inter-chain disulfide linkages between dimers and multimers are known to be responsible for stabilizing the three-dimensional structure of mature HBsAg particles, playing a key role in determining their antigenicity, similar to the plasma-derived antigen [35]. Moreover, it has been proposed that the building block of VLPs is a dimer of HBsAg [36].

To evaluate the ability of the VLPs to bind to anti-HBs antibodies, and thereby to evaluate the performance of the latest generation of HBsAg detection assays with respect to rHBsAg from subgenotypes A2, F1b, F4 and the G145R mutant, two commercial assays were tested. Both assays, Elecsys HBsAg II and ARCHITECT HBsAg, showed a reduction in the antigen detection signal with the VLPs containing HBsAg from subgenotype F1b, and an even more pronounced reduction in the HBsAg detection signal was observed with the VLPs containing the G145R mutant in comparison with those from genotype A.

In contrast to the ARCHITECT HBsAg assay, whose detection values for HBsAg from subgenotype F4 were almost 20% higher than those obtained with genotype A, the Elecsys assay showed a weaker antigen detection signal (almost 32% lower than that obtained with genotype A). Similar results were achieved with VLPs purified from serum samples obtained from patients with chronic HBV of subgenotypes A2, F1b and F4.

These results indicate a need for novel diagnostic immunoassays that efficiently detect HBV genotype F and S-escape mutants, at least in geographical areas where the Amerindian genotype is endemic.

A similar approach for the development of novel anti-hepatitis B vaccines should be considered.

Table 1 Local RMSD values

Sequence region	A2wt A2mut	A2wt F1b	A2wt F4	F1b F4
Global	2.63	4.06	1.97	4.01
Residues 1-39 (including helix α1)	2.04	2.48	2.22	2.43
Residues 40-79 (cytoplasmic loop)	3.95	3.33	1.99	3.06
Residues 80-100 (corresponding to helix α3)	0.66	0.60	0.55	0.53
Residues 101-160 (MHR)	2.84	4.04	1.80	4.16
Residues 161-226 (including helix α4 and helix α5)	1.40	1.67	1.31	1.47

The influence of the high genetic variability of HBV on the sensitivity of serological and molecular assays has received little attention so far. As mentioned above, a major source of variability is related to viral genotypes and subgenotypes. There have been few reports about the sensitivities of the different HBsAg screening assays for HBV subtypes or genotypes and mutants, and few studies have investigated the dependence of the analytical sensitivity of HBsAg assays on the genotype or subtype [37–39]. Furthermore, the possible influence of a particular genotype on diagnosis and prophylaxis has mostly been evaluated for genotypes A, B, C and D, and there is still a lack of robust data showing the efficiency of detection of HBsAg from HBV genotype F. The significant variation between the two commercial diagnostic assays observed in this study, in which the highest variability was observed for subgenotype F1b (150%), highlights the implications of using different diagnostic kits in specific geographical areas.

HBsAg detection using monoclonal antibodies may be unreliable in populations where circulating subtypes/genotypes or variants are distinct from the virus strain used in the production of these antibodies (i.e., genotype A). The MHR of genotype F is more divergent than that of genotype A, with a divergence of five and six distinct amino acids for subgenotypes F4 and F1b, respectively (Fig. 4). The four predicted 3D structures were similar, with global root mean square deviation (RMSD) values between the selected pairs of genotypes that were in a range of 1.97 to 4.06 (Table 1). An analysis of local RMSD values showed that the cytoplasmic loop and the MHR were the most structurally divergent regions, whereas the membrane-anchoring elements (transmembrane helices α1, α3, α4 and α5) were structurally more conserved (Table 1). The predicted conformational changes (Fig. 5) support the anti-HBs binding data, suggesting that subgenotypes F1b and F4 do not behave as escape mutants but cause a decrease in the binding to the anti-HBs antibodies used for diagnosis. In this regard, it has been reported that variations located outside of or close to the "a" determinant might induce changes in the structural configuration so that HBV cannot be efficiently neutralized by anti-HBs antibodies but still be recognized by them [40].

Thus, an important question is whether the diagnostic reagents initially developed for genotype A strains are also suitable for the detection of genotype F infections. In addition, current HBV vaccines based on genotypes A and D may not be fully protective against infections caused by HBV genotype F. In this regard, 'protective' anti-HBs antibodies, generated against HBsAg from genotype A and D in recombinant vaccines, may possibly not confer sufficient protection against infections caused by HBV genotype F.

Because of the quasispecies nature of HBV, mixed-genotype infection and intergenotypic recombination are not uncommon, thus explaining why most of the commercial diagnostic kits guarantee a reliable detection of the G145R mutant, for example, using sera of acutely or chronically infected patients as test samples.

Thus, the performance of HBsAg immunoassays in terms of genotype and surface antigen variability needs to be further improved for a better diagnosis of HBV infection.

These data emphasize the need to conduct further studies to better characterize and understand the different aspects of genotype F, especially in relation to diagnosis and prophylaxis.

Finally, the newly synthesized VLPs obtained in this study are a useful means of testing the robustness of commercial HBsAg assays. Most importantly, these newly synthesized antigens might also allow an improved diagnosis and prophylaxis of HBV infection.

Acknowledgements DGN, ADN, PDG, CSC and MLC are staff members of CONICET. MJL thanks CONICET for her doctoral scholarship.

Funding This study was funded by the University of Buenos Aires (Grant UBACyT 20020130200222BA) and by the Agencia Nacional de Promoción Científica y Técnica (ANPCyT, Grant PICT 201-0206).

Compliance with ethical standards

Conflict of interest The authors declare that they have no conflicts of interest regarding funding or other aspects of this manuscript.

Ethical approval The study was approved by the institutional review committee at Facultad de Farmacia y Bioquímica, Universidad de Buenos Aires (Ref. EXP- UBA N" 0051009/2016).

References

1. WHO (2017) Hepatitis B. World Health Organization Fact sheet N°204. http://www.who.int/mediacentre/factsheets/fs204/en. Accessed 9 Apr 2018
2. Kramvis A (2014) Genotypes and genetic variability of hepatitis B virus. Intervirology 57:141–150. https://doi.org/10.1159/000360947
3. Lin CL, Kao JH (2017) Natural history of acute and chronic hepatitis B: the role of HBV genotypes and mutants. Best Pract Res Clin Gastroenterol 31:249–255. https://doi.org/10.1016/j.bpg.2017.04.010
4. Croagh CMN, Desmond PV, Bell SJ (2015) Genotypes and viral variants in chronic hepatitis B: a review of epidemiology and clinical relevance. World J Hepatol 7(3):289–303. https://doi.org/10.4254/wjh.v7.i3.289
5. Pourkarim MR, Amini-Bavil-Olyaee S, Kurbanov F, Van Ranst M, Tacke F (2014) Molecular identification of hepatitis B virus genotypes/subgenotypes: revised classification hurdles and updated resolutions. World J Gastroenterol 20(23):7152–7168
6. Alvarado-Mora MV, Rebello Pinho JR (2013) Distribution of HBV genotypes in Latin America. Antivir Ther 18:459–465. https://doi.org/10.3851/IMP2599
7. Sanchez-Tapias JM, Costa J, Mas A, Bruguera M, Rodes J (2002) Influence of hepatitis B virus genotype on the long-term

outcome of chronic hepatitis B in Western patients. Gastroenterology 123:1848–1856
8. Livingston SE, Simonetti J, McMahn BJ, Bulkow LR, Hurlburt KJ, Homan CE, Snowball MM, Cagle HH, Williams JL, Chulanov VP (2007) Hepatitis B virus genotypes in Alaska Native people with hepatocellular carcinoma: preponderance of genotype F. J Infect Dis 195:5–11
9. Marciano S, Galdamo OA, Gadano AC (2013) HBV genotype F: Natural history and treatment. Antivir Ther 18:485–488. https://doi.org/10.3851/IMP2604
10. Cassidy A, Mossman S, De Ridder M, Leroux-Roels G (2011) Hepatitis B vaccine effectiveness in the face of global HBV genotype diversity. Expert Rev Vaccines 10(12):1709–1715. https://doi.org/10.1586/erv.11.151
11. Tacke F, Amini-Bavil-Olyaee S, Heim A, Luedde T, Manns MP, Trautwein C (2007) Acute hepatitis B virus infection by genotype F despite successful vaccination in an immune-competent German patient. J Clin Virol 38:353–357
12. O'Halloran JA, De Gascun CF, Dunford L, Carr MJ, Connell J, Howard R, Hall WW, Lambert JS (2011) Hepatitis B virus vaccine failure resulting in chronic hepatitis B infection. J Clin Virol 52:151–154. https://doi.org/10.1016/j.jcv.2011.06.020
13. Xiao A, Zhou X, Zhou L, Zhang Y (2006) Improvement of cell viability and hirudin production by ascorbic acid in *Pichia pastoris* fermentation. Appl Microbiol Biotechnol 72:837–844
14. Celik E, Calık P, Oliver S (2009) Fed-batch methanol feeding strategy for recombinant protein production by *Pichia pastoris* in the presence of co-substrate sorbitol. Yeast 26:473–484
15. Bhatacharya P, Pandey G, Mukherjee KJ (2007) Production and purification of recombinant human granulocyte-macrophage colony stimulating factor (GM-CSF) from high cell density cultures of *Pichia pastoris*. Bioprocess Biosyst Eng 30:305–312
16. Noseda DG, Recúpero MN, Blasco M, Ortiz GE, Galvagno MA (2013) Cloning, expression and optimized production in a bioreactor of bovine chymosin B in *Pichia* (*Komagataella*) *pastoris* under *AOXI* promoter. Protein Expr Purif 92:235–244. https://doi.org/10.1016/j.pep.2013.08.018
17. Noseda DG, Blasco M, Recúpero MN, Galvagno MA (2014) Bioprocess and downstream optimization of recombinant bovine chymosin B in *Pichia* (*Komagataella*) *pastoris* under methanol-inducible *AOXI* promoter. Protein Expr Purif 104:85–91. https://doi.org/10.1016/j.pep.2014.09.014
18. Bardiya N (2006) Expression in and purification of hepatitis B surface antigen (S-protein) from methylotrophic yeast *Pichia pastoris*. Anaerobe 12:194–203
19. Gurramkonda C, Zahid M, Nemani SK, Adnan A, Gudi SK, Ebensen T, Lünsdorf H, Guzmán CA, Rinas U (2013) Purification of hepatitis B surface antigen virus-like particles from recombinant *Pichia pastoris* and in vivo analysis of their immunogenic properties. J Chromatogr B Analyt Technol Biomed Life Sci 940:104–111. https://doi.org/10.1016/j.jchromb.2013.09.030
20. Peyret H (2015) A protocol for the gentle purification of virus like particles produced in plants. J Virol Methods 225:59–63. https://doi.org/10.1016/j.jviromet.2015.09.005
21. Drozdetskiy A, Cole C, Procter J, Barton GJ (2015) JPred4: a protein secondary structure prediction server. Nucleic Acids Res 43(W1):W389–W394. https://doi.org/10.1093/nar/gkv332
22. Yang J, Yan R, Roy A, Xu D, Poisson J, Zhang Y (2015) The I-TASSER Suite: Protein structure and function prediction. Nat Methods 12:7–8. https://doi.org/10.1038/nmeth.3213
23. Laskowski RA, MacArthur MW, Moss D, Thornton JM (1993) PROCHECK: a program to check the stereochemical quality of protein structures. J Appl Crystallogr 26:283–291
24. Studer G, Biasini M, Schwede T (2014) Assessing the local structural quality of transmembrane protein models using statistical potentials (QMEANBrane). Bioinformatics 30(17):i505–i511. https://doi.org/10.1093/bioinformatics/btu457
25. Wiederstein M, Sippl MJ (2007) ProSA-web: interactive web service for the recognition of errors in three-dimensional structures of proteins. Nucleic Acids Res 35:W407–W410
26. Xu D, Zhang Y (2011) Improving the physical realism and structural accuracy of protein models by a two-step atomic-level energy minimization. Biophys J 101:2525–2534. https://doi.org/10.1016/j.bpj.2011.10.024
27. Lomize MA, Pogozheva ID, Joo H, Mosberg HI, Lomize AL (2012) OPM database and PPM web server: resources for positioning of proteins in membranes. Nucleic Acids Res 40(Database issue):D370–D376. https://doi.org/10.1093/nar/gkr703
28. Holm L, Rosenström P (2010) Dali server: conservation mapping in 3D. Nucleic Acids Res 38:W545–W549. https://doi.org/10.1093/nar/gkq366
29. Pettersen EF, Goddard TD, Huang CC, Couch GS, Greenblatt DM, Meng EC, Ferrin TE (2004) UCSF Chimera—a visualization system for exploratory research and analysis. J Comput Chem 25(13):1605–1612
30. Milhiet P-E, Dosset P, Godefroy C, Le Grimellec C, Guigner J-M, Larquet E, Ronzon F, Manin C (2011) Nanoscale topography of hepatitis B antigen particles by atomic force microscopy. Biochimie 93:254–259. https://doi.org/10.1016/j.biochi.2010.09.018
31. Lündsorf H, Gurramkonda C, Adnan A, Khanna N, Rinas U (2001) Virus-like particle production with yeast: ultrastructural and immunocytochemical insights into *Pichia pastoris* producing high levels of the hepatitis B surface antigen. Microb Cell Fact 10:48
32. Wampler DE, Lehman ED, Boger J, McAleer WJ, Scolnick EM (1985) Multiple chemical forms of hepatitis B surface antigen produced in yeast. Proc Natl Acad Sci USA 82:6830–6834
33. Zhao Q, Wang Y, Freed D, Fu T-M, Gimenez JA, Sitrin RD, Washabaugh MW (2006) Maturation of recombinant hepatitis B virus surface antigen particles. Hum Vaccin 2(4):174–180
34. Zahid M, Lündsorf H, Rinas U (2015) Assessing stability and assembly of the hepatitis B surface antigen into virus-like particles during down-stream processing. Vaccine 33:3739–3745. https://doi.org/10.1016/j.vaccine.2015.05.066
35. Ottone S, Nguyen X, Bazin J, Bérard C, Jimenez S, Letourneur O (2007) Expression of hepatitis B surface antigen major subtypes in *Pichia pastoris* and purification for *in vitro* diagnosis. Protein Expr Purif 56:177–188
36. Gilbert RJ, Beales L, Blond D, Simon MN, Lin BY, Chisari FV, Stuart DI, Rowlands DJ (2005) Hepatitis B small surface antigen particles are octahedral. Proc Natl Acad Sci USA 102(41):14783–14788
37. Olinger CM, Weber B, Otegbayo JA, Ammerlaan W, van der Taelem-Brulé N, Muller CP (2007) Hepatitis B virus genotype E surface antigen detection with different immunoassays and diagnostic impact of mutations in the preS/S gene. Med Microbiol Immunol 196:247–252
38. Araujo NM, Vianna COA, Morales MTB, Gomes SA (2009) Expression of hepatitis B virus surface antigen (HBsAg) from genotypes A, D and F and influence of amino acid variations related or not to genotypes on HBsAg detection. Braz J Infect Dis 13:266–271
39. Scheiblauer H, El-Nageh M, Diaz S, Nick S, Zeichhardt H, Grunet H-P, Prince A (2010) Performance evaluation of70 hepatitis B virus (HBV) surface antigen (HBsAg) assays from around the world by a geographically diverse panel with an array of HBV genotypes and HBsAg subtypes. Vox Sang 98:403–414. https://doi.org/10.1111/j.1423-0410.2009.01272.x

40. Hadiji-Abbes N, Mihoubi W, Martin M, Karakasyan-Dia C, Frikha F, Gergely C, Jouenne T, Gargouri A, Mokdad-Gargouri R (2015) Characterization of C69R variant HBsAg: effect on bindingto anti-HBs and the structure of virus-like particles. Arch Virol 160:2427–2433. https://doi.org/10.1007/s00705-015-2515-y